

# Direct Photon-counting Scintillation Detector Readout using an SSPM

Christopher J. Stapels<sup>\*, a</sup>, Michael R. Squillante,<sup>a</sup> Frank L. Augustine,<sup>b</sup> and James F. Christian<sup>a</sup>

<sup>a</sup>Radaition Monitoring Devices, 44 Hunt Street, Watertown, MA 02054, USA

<sup>b</sup>Augustine Engineering, 2115 Park Dale Ln, Encinitas, CA 92024, USA

**Elsevier use only:** Received date here; revised date here; accepted date here

## Abstract

Gamma-ray detector technologies, capable of providing adequate energy information, use photomultiplier tubes (PMTs) or silicon avalanche photodiodes to detect the light pulse from a scintillation crystal. A new approach to detect the light from scintillation materials is to use an array of small photon counting detectors, or a “detector-on-a-chip” based on a novel “Solid-state Photomultiplier” (SSPM) concept. A CMOS SSPM coupled to a scintillation crystal uses an array of CMOS Geiger photodiode (GPD) pixels to collect light and produce a signal proportional to the energy of the radiation. Each pixel acts as a binary photon detector, but the summed output is an analog representation of the total photon intensity. We have successfully fabricated arrays of GPD pixels in a CMOS environment, which makes possible the production of miniaturized arrays integrated with the detector electronics in a small silicon chip. This detector technology allows for a substantial cost reduction while preserving the energy resolution needed for radiological measurements.

In this work, we compare designs for the SSPM detector. One pixel design achieves maximum detection efficiency for 632-nm photons approaching 30% with a room temperature dark count rate of less than 1 kHz for a 30- $\mu\text{m}$ -diameter pixel. We characterize after pulsing and optical cross talk and discuss their effects on the performance of the SSPM. For 30- $\mu\text{m}$  diameter, passively quenched CMOS GPD pixels, modeling suggests that a pixel spacing of approximately 90  $\mu\text{m}$  optimizes the SSPM performance with respect to detection efficiency and cross-talk.

© 2001 Elsevier Science. All rights reserved

**Keywords:** Dosimeter; nuclear; radiation; detector; GPD; APD; SSPM;

## 1. Introduction

Although scintillating materials are ideal for detecting and measuring high-energy radiation, the limitations of existing optical detectors reduces their functionality. An appropriate CMOS photomultiplier technology would provide a fully integrated, low-cost solution to optimize the functionality of scintillation materials, which is essential for applications such as the development of deployable digital dosimeters and radiation spectrometers.

An SSPM is an array of avalanche photodiodes operating in Geiger mode, referred to as Geiger photodiodes (GPDs). The SSPM achieves the low noise of a PMT at a low cost

while retaining the high quantum efficiency of a silicon device when coupled to a scintillation detector. Figure 1 illustrates the principle of operation of the SSPM.

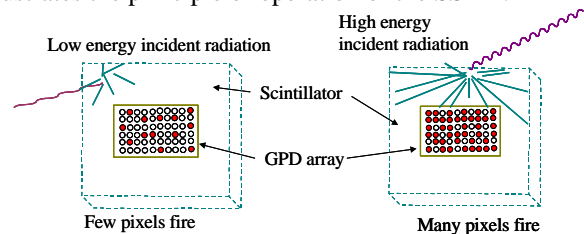


Figure 1: SSPM principal of operation. Nuclear photons strike the scintillation crystal and produce visible light proportional to their energy. The number of pixels that fire in the GPD array is thus a function of the incident energy.

The light produced in the scintillation material is proportional to the energy of the absorbed event, the

\* Corresponding author. Tel.: 617-668-6896; fax: 617-668-6891; e-mail: cstapels@rmdinc.com.

number of pixels that fire provides the energy of the incident photon when the SSPM is uniformly illuminated.

P. Buzhan *et al.* have shown that this method approaches and exceeds the performance of a standard PMT for detection of the optical scintillation photons in certain applications [1]. Implementing this approach in a CMOS compatible process will allow high precision, low-cost, sensors with the additional benefit of integration of signal processing electronics right on the chip. We have fabricated several CMOS-based test arrays of these pixel sensors and characterized their performance as individual detectors, and as arrays [2-5]. Figure 2 shows a photograph of a test chip that contains 3 test arrays with three different pixel pitches.



**Figure 2.** First array chip, designated AE-189. The chip contains three nine-element arrays, and eight active quenching circuits. The arrays have 60, 80 and 150-micron spacing; each array has two independent elements and seven summed elements. Test pixels with various sizes are included on the left.

In the SSPM, the individual pixels are biased above their reverse-bias breakdown voltage, which is referred to as Geiger-mode operation. Various aspects of the performance and operation of GPD pixels, fabricated with custom processes, have been studied [6-12]. The design of the CMOS pixel described in this work, specifically referred to as design 12, is similar to that of Rochas *et al.* [13].

In this work, we are interested in the following list of SSPM performance characteristics:

- 1 SSPM detection efficiency (DE)
- 2 SSPM intensity range and energy resolution
- 3 SSPM sensitivity

Individual pixel characteristics affect the performance of the SSPM, such as the pixel DE, after pulsing in the pixel, and cross talk between pixels. In general, Geiger pulses typically exhibit very good pulse height uniformity, so effects of Geiger pulse height variations are relatively negligible.

## 2. Methods

Readily measured characteristics of the CMOS GPD pixels can be used to model the SSPM performance in order to optimize the design. The following list summarizes these characteristics: the size of the pixel, the size of the array, the fill-factor, the operating bias, the detection efficiency (DE) of the GPD pixel, the dark count rate (DCR) of the GPD pixels in the array, the fill factor, the after pulsing gain factor, and the cross talk gain factor.

In general, diodes are connected so that the anode is held at ground and the cathode is biased through an 80-k $\Omega$  resistor. The Geiger voltage is measured via AC coupling on the cathode connection. The measurement of radiometric performance has been previously described [2-4]. Pixels are initially characterized by the detection efficiency (DE) and by the rate of dark events.

Both the after pulsing and cross talk can be characterized by an effective multiplication factor,  $M_a$  and  $M_x$ , respectively [5]. In this work, we measure the cross talk gain factor between a pair of pixels,  $m_x$ , as a function of bias and pixel spacing; we then extrapolate the cross talk gain factor of the SSPM,  $M_x$ , which is described in more detail in [5]. Equation (1) defines the pair wise cross talk probability,  $P_x$ .

$$P_x = 1 - \frac{1}{m_x} = 1 - \frac{i_1 + i_2}{I_1 + I_2}, \quad (1)$$

where  $I_1$  and  $I_2$  refer to the count rate in pixels 1 and 2, respectively, when both pixels are operating simultaneously. The symbols  $i_1$  and  $i_2$  refer to the count rate of the isolated pixel, which is measured when the other pixel is unbiased. In addition, we assume that a simple phenomenological function, defined in Equation (2), describes the dependence of the cross talk on the excess bias and pixel spacing.

$$P_x \cong \frac{\alpha V_x}{r^2}, \quad (2)$$

where  $\alpha$  is a constant recovered from a fit to the data, and  $r$  is the distance between the pixels.

## 3. Results and Discussion

### 3.1. Single pixel detection efficiency and after pulsing

Figure 3 shows the bias dependence of the apparent DE, which includes after pulses, and the 632-nm DE referenced to the axis on the left.

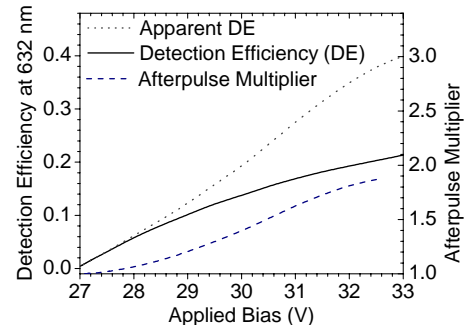


**Figure 3** The single optical photon detection efficiency (DE). The measured “Apparent DE” is corrected with the measured after pulse multiplier.

The figure also plots the bias dependence of the after pulse multiplier,  $M_a$ , referenced to the axis on the right. The DE

is the product of quantum efficiency and Geiger probability. Our measured DE of  $\sim 22\%$  indicates a Geiger breakdown probability of  $\sim 90\%$  because the QE at 632-nm for the design-12 pixel is  $\sim 30\%$ . The detection efficiency of the SSPM is the DE of the pixel times the fill factor of the array, which is the ratio of active area to the total area of the SSPM. In our small SSPM prototypes, the SSPM fill factor ranges from 20% to 3%.

### 3.2. Cross talk

One study has shown theoretical calculations indicating that cross talk, or interference from adjacent pixels can become an issue at distances below 400 microns [14]. The pair wise cross talk probability described in equation (1) is plotted for pixels at a spacing of 60 microns, 78.7 microns and 150 microns in Figure 4. For all the measured values, the curves approximately follow a  $1/r^2$  function, as expected.

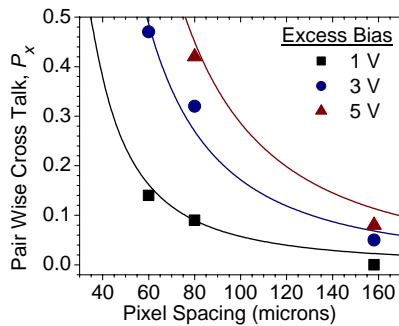


Figure 4 Cross talk as a function of spacing for three values of excess bias. The excess bias is the bias voltage minus the reverse bias breakdown voltage. The dashed lines represent a simple  $1/r^2$  function fitted to the data points.

The cross talk depends on the hot-carrier emission [15-17] of the offending pixels and the detection efficiency of the receiving pixel. The detection efficiency in this case is the measured DE scaled by a geometric efficiency factor that is a constant of the bias. Comparison of the cross talk probability and the detection efficiency will give some indication of the emission of the offending pixel. The cross talk gain as a function of bias for one array at 78.7 microns is shown in Figure 5.

Both the cross talk and detection efficiency increase with the applied bias. The ratio of  $P_x/DE$  gives some indication of the emission behaviour from the Geiger pixels. The increase in the ratio with increasing bias suggests that the hot-carrier emission from the pixels increases with increasing bias. The more recent values for the pair wise cross talk plotted in Figure 5 are roughly a factor-of-two smaller than those plotted in Figure 4. The more recent values are encouraging, however, we are still investigating the source of the discrepancy.

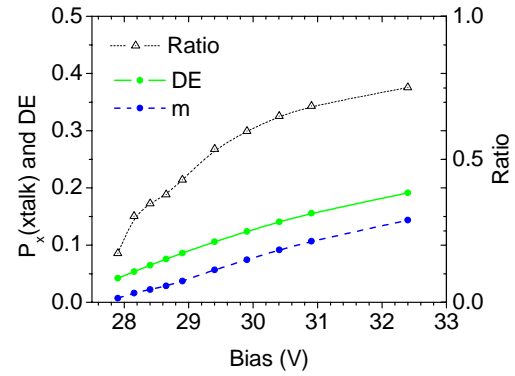


Figure 5 The bias dependence of the pair wise cross talk and the DE for pixels spaced at 78.7 microns. The ratio of  $P_x/DE$  estimates the bias dependence of the hot-carrier emission from the Geiger pixel.

### 3.3. Model results

The purpose of the modeling is to estimate the anticipated performance of the SSPMs with different pixel spacing when operated at various bias conditions. The pixel spacing and bias conditions affect the SSPM DE and the SSPM energy resolution through the cross talk. The cross talk causes the pixels to fire in bunches, which lowers the effective number of pixels in the detector, and thus the SSPM energy resolution.

The modeling [5] shows a trade-off between maximizing the SSPM DE by reducing the spacing, i.e., increasing the fill factor, and the amount of cross talk, which reduces the energy resolution. It also shows a weak dependence of the SSPM DE on the fill factor and operating voltage because SSPMs with lower fill factors can be operated at higher bias voltages, and *vice versa*, to obtain the same energy resolution performance. In summary, the modeling suggests that a 2mm x 2mm CMOS SSPM is optimized when the spacing of the 30-micron diameter pixels is  $\sim 90$  microns, and when it is operated at an excess bias of 0.5, it will provide  $\sim 230$  effective pixels.

### 3.4. Prototype CMOS SSPM

We have fabricated small prototype CMOS SSPM detectors. Figure 6 shows a photograph of a 4x20-pixel SSPM, with 20-micron diameter pixels at a spacing of 46 microns.



Figure 6 Photograph of a prototype CMOS SSPM detector. The array consists of 100 pixels, 4x25, each with a diameter of 20 microns, spaced at a distance of 46 microns.

For our initial performance characterization, we have measured the proportionality of the response to a pulsed

632-nm diode laser. Placing neutral-density filters between the diode laser and the SSPM detector decreases the intensity of the light pulse. Figure 7 plots the pulse height spectrum obtained from the 100-pixel SSPM at various illumination intensities.

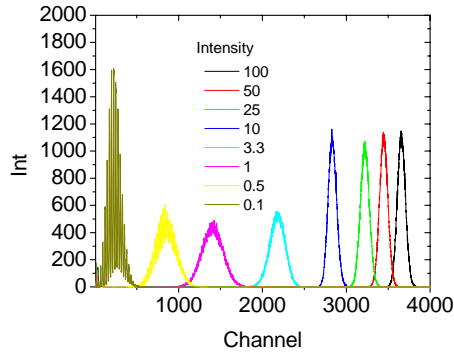


Figure 7: 100-pixel spectrum of array output with varying incident light. The pixel pitch is 46 microns and the excess bias, which is the bias above the breakdown voltage, is 0.6 volts. Peaks farther along the x – axis represent more pixels firing simultaneously, due to a higher photon flux in the crystal. The dark counts are suppressed due to a voltage dependant gate applied to the MCA.

The signal from the individual Geiger pixels can be resolved for the smallest light intensity, 0.1, in the figure. As the intensity of the light increases, the signals from the individual pixels overlap, to produce a single peak whose mean position increases with an increasing number of photons in the light pulse. The scale relating the intensity to the mean position in this preliminary measurement is not linear. The non-linearity may also cause the width of the peaks in the figure to decrease when the light intensity increases.

### 3.5. Scintillation detector readout

We used the prototype SSPM, photographed in Figure 7, to readout a 1mm x 1mm x 5 mm CsI(Tl)scintillation crystals. Figure 8 shows the pulse height spectra from the CMOS SSPM when exposed to radiation from a  $^{57}\text{Co}$  source at 122 keV and a  $^{22}\text{Na}$  source at 511 keV.

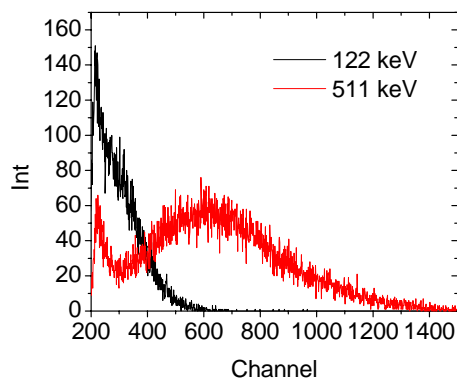


Figure 8 Pulse height spectra measured with a 1mm x 1mm x 5mm CsI(Tl) crystal coupled to the 4x25-element SSPM when exposed to radiation from  $^{57}\text{Co}$ , 122 keV, and  $^{22}\text{Na}$ , 511 keV.

These results are very preliminary, however, encouraging. The mismatch between the open area of the scintillation crystal, 1mm x 1mm, and the area of the CMOS SSPM, 0.2 mm x 1 mm introduces substantial optical coupling losses. The reflective aluminium of the SSPM only recovers a fraction of this loss. Matching the size of the SSPM detector to the open area of the scintillation detector optimizes the optical coupling and light collection of the detector.

## 4. Conclusions

Among the host of factors that control the performance of an SSPM, cross talk and after pulsing are most significant at the bounds of device sensitivity. We have performed initial measurements of these parameters and used them to guess wildly. New devices with higher pixel numbers and larger active areas promise to provide improves performance.

## 5. References

- [1] P. Buzhan, B. Dolgoshein, L. Filatov, A. Ilyin, V. Kantzerov, V. Kaplin, A. Karakash, F. Kayumov, S. Klemin, E. Popova, and S. Smirnov, "Silicon photomultiplier and its possible applications," *Nuclear Instruments and Methods in Physics Research, Section A*, vol. 504, pp. 48-52, 2003.
- [2] J. F. Christian, G. Svolos, A. I. Kogan, F. L. Augustine, M. R. Squillante, and G. Entine, "Characterization & Modeling of APD Pixels Made with CMOS Technology," presented at Nano Materials for Defense Applications, Maui, HI, 2004.
- [3] C. Stapels, W. G. Lawrence, M. R. Squillante, G. Entine, F. L. Augustine, and J. Christian, "The Solid-state Photomultiplier for an Improved Gamma-ray Detector," presented at IEEE Conference on Technologies for Homeland Security (1105) April 26-28, Boston, MA, 2005.
- [4] C. J. Stapels, W. G. Lawrence, F. L. Augustine, and J. F. Christian, "Characterization of a CMOS Geiger Photodiode Pixel," *IEEE Transactions on Electron Devices*, vol. 53, pp. 631, 2006.
- [5] C. J. Stapels, W. G. Lawrence, F. L. Augustine, and J. F. Christian, "CMOS Solid-State Photomultiplier for Detecting Scintillation Light in Harsh Environments," presented at SNIC Symposium (<http://www-conf.slac.stanford.edu/snic/proceedings/status.htm>), SLAC Stanford, CA, 2006.
- [6] S. Cova, M. Ghioni, A. Lacaita, C. Samori, and F. Zappa, "Avalanche photodiodes and quenching circuits for single-photon detection," *Appl. Opt.*, vol. 35, pp. 1956, 1996.
- [7] S. Cova, A. Lacaita, and G. Ripamonti, "Trapping phenomena in avalanche photodiodes on nanosecond scale," *IEEE Electron Device Lett. (USA)*, vol. 12, pp. 685-7, 1991.
- [8] S. Vasile, P. Gothoskar, R. Farrell, and D. Sdrulla, "Photon detection with high gain avalanche photodiode arrays," *IEEE Trans. Nucl. Sci. (USA)*, vol. 45, pp. 720-3, 1998.
- [9] W. J. Kindt and H. W. Van Zeijl, "Modelling and fabrication of Geiger mode avalanche photodiodes," *IEEE Trans. Nucl. Sci. (USA)*, vol. 45, pp. 715-19, 1998.
- [10] E. Sciacca, A. C. Giudice, D. Sanfilippo, F. Zappa, S. Lombardo, R. Consentino, C. Di Franco, M. Ghioni, G. Fallica, G. Bonanno, S. Cova, and E. Rimini, "Silicon Planar Technology for Single-Photon Optical Detectors," *IEEE Trans. Electron Devices*, vol. 50, pp. 918-25, 2003.
- [11] B. F. Aull, A. H. Loomis, D. J. Young, R. M. Heinrichs, B. J. Felton, P. J. Daniels, and D. J. Landers, "Geiger-mode avalanche

- photodiodes for three-dimensional imaging," *Linc. Lab. J. (USA)*, vol. 13, pp. 335-50, 2002.
- [12] J. C. Jackson, A. P. Morrison, D. Phelan, and A. Mathewson, "A novel silicon Geiger-mode avalanche photodiode," presented at International Electron Devices Meeting. Technical Digest (Cat. No.02CH37358), 2002.
- [13] A. Rochas, M. Gani, B. Furrer, P. A. Besse, R. S. Popovic, G. Ribordy, and N. Gisin, "Single photon detector fabricated in a complementary metal-oxide-semiconductor high-voltage technology," *Rev. Sci. Instrum. (USA)*, vol. 74, pp. 3263-70.
- [14] J. C. Jackson, D. Phelan, A. P. Morrison, R. Redfern, and A. Mathewson, "Characterization of Geiger mode avalanche photodiodes for fluorescence decay measurements," *Proc. SPIE - Int. Soc. Opt. Eng. (USA)*, vol. 4650, pp. 55-66, 2002.
- [15] A. L. Lacaita, F. Zappa, S. Bigliardi, and M. Manfredi, "On the bremsstrahlung origin of hot-carrier-induced photons in silicon devices," *IEEE Trans. Electron Devices (USA)*, vol. 40, pp. 577-82, 1993.
- [16] L. Carbone, R. Brunetti, C. Jacoboni, A. Lacaita, and M. Fischetti, "Polarization analysis of hot-carrier light emission in silicon," *Semicond. Sci. Technol. (UK)*, vol. 9, pp. 674-6, 1994.
- [17] S. Villa, A. L. Lacaita, and A. Pacelli, "Photon emission from hot electrons in silicon," *Phys. Rev. B, Condens. Matter (USA)*, vol. 52, pp. 10993-9, 1995.